

The large-scale smoothness of the Universe

Kelvin K. S. Wu, Ofer Lahav & Martin J. Rees

The Universe is inhomogeneous—and essentially fractal—on the scale of galaxies and clusters of galaxies, but most cosmologists believe that on larger scales it becomes isotropic and homogeneous: this is the ‘cosmological principle’. This principle was first adopted when observational cosmology was in its infancy, and was then little more than a conjecture. The data now available offer a quantitative picture of the gradual transition from small-scale fractal behaviour to large-scale homogeneity.

A fractal is a distribution or shape that is not homogeneous (in general), but possesses the property that each part is a simulacrum of the whole. In other words it ‘looks’ the same on all scales. Fractals abound in nature: for example, the coastline of a small peninsula drawn on paper could equally well depict a large continent; and fractals have long been studied as manifestations of scaling laws in solid-state physics^{1,2}. The clustering of galaxies (see Fig. 1) lends itself to a fractal description^{1–7}, because the clumpiness prevails over a wide range of scales. The big question for cosmology is whether the distribution of matter continues to be a simple fractal beyond the scale of clusters of galaxies: if it does, then the cosmological principle is invalid.

Past attempts to determine the distribution of matter have confronted two important obstacles. Most of the mass in the Universe is dark; we can detect it only by its gravitational effect on objects that we can see, and it is still unclear how to relate the distributions of light and mass. In particular, we have not known how to match the clustering of galaxies with the cosmic microwave background (CMB) anisotropies, which tell us about the mass fluctuations in the early Universe. In addition, little has been known about fluctuations in the distribution of matter on scales intermediate between those of local galaxy surveys ($\leq 100 h^{-1}$ Mpc, where h is the Hubble constant in units of $100 \text{ km s}^{-1} \text{ Mpc}^{-1}$) and scales probed by the Cosmic Background Explorer (COBE) satellite ($\geq 1,000 h^{-1}$ Mpc).

Recent observations of radio galaxies and the X-ray background (XRB, which probably arises from distant active galactic nuclei), at median redshift $\bar{z} \approx 1$, can now effectively probe these intermediate scales. Moreover, experiments to measure fluctuations in the microwave background on smaller angular scales than those probed by COBE are also helping to bridge the gap. Future surveys of more than one million galaxies will probe to a median redshift $\bar{z} \approx 0.1$ (which roughly corresponds to a co-moving distance of $\sim 300 h^{-1}$ Mpc). Current data, however, already strongly constrain any non-uniformities in the galaxy distribution (as well as the overall mass distribution) on scales $\geq 300 h^{-1}$ Mpc.

In the language of fractals (see Box 1), fractal dimensions are used to characterize the degree of clustering; these generalize our intuitive concepts of dimension and can take any positive value less than or equal to 3. On scales below $\sim 10 h^{-1}$ Mpc, galaxies are distributed with the correlation dimension⁸ $D_2 = 1.2\text{--}2.2$ (Box 1 and Table 1). But we show below that on large scales D_2 is very close to the homogeneous value of 3. Any quantitative discussion of the large-scale structure in the Universe in fact depends on the unknown cosmological parameters (defined only for a homogeneous and isotropic universe): the density parameter Ω , the cosmological constant Λ and the Hubble constant H_0 . For simplicity we present the observational results interpreted for the Einstein-de Sitter model ($\Omega = 1$ and $\Lambda = 0$), but the main conclusions are not altered for other models.

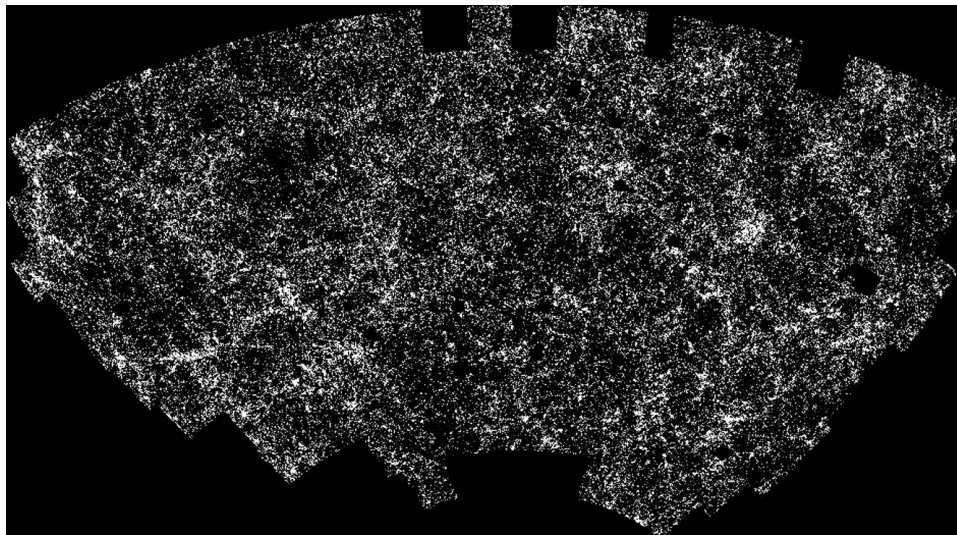


Figure 1 The distribution of 2 million galaxies with blue magnitude $17 \leq b_j \leq 20.5$ shown in an equal-area projection centred on the south Galactic pole. The data are from scans over a contiguous area of 4,300 square degrees using the Automatic Plate Measuring (APM) machine¹⁰. The small empty patches in the

map are regions excluded around bright stars, nearby dwarf galaxies, globular clusters and regions removed for calibration purposes. Although projection and superposition effects tend to wash out three-dimensional structures, the pattern is seen to be non-uniform, with clusters, filaments and voids.

Box 1 The fractal dimension

If we count, for each galaxy, the number of galaxies within a distance R from it, and call the average number obtained $N(<R)$, then the distribution is said to be a fractal of correlation dimension D_2 if $N(<R) \propto R^{D_2}$. Of course D_2 may be 3, in which case the distribution is homogeneous rather than fractal. In the pure fractal model, this power law holds for all scales of R , whereas in a hybrid model it holds for R less than some scale, above which D_2 increases towards 3 to accommodate the cosmological principle. To allow for varying D_2 one often writes:

$$D_2 = \frac{d(\ln N(<R))}{d(\ln R)}$$

Using the above, the fractal proponents^{4,5} have estimated $D_2 \approx 2$ for all scales up to $\sim 1,000 h^{-1}$ Mpc, whereas other groups^{6,18,66-70} have obtained, in general, scale-dependent values as listed in Table 1.

These measurements can be directly compared with the popular cold dark matter (CDM) models of density fluctuations, which predict the increase of D_2 with R . If we now assume homogeneity on large scales, then the mean density \bar{n} and the correlation function $\xi(r)$ can be defined, and:

$$N(<R) = \frac{4\pi}{3} R^3 \bar{n} + 4\pi \bar{n} \int_0^R dr r^2 \xi(r)$$

for a flat universe with $\Omega = 1$. Hence we have a direct mapping between ξ and D_2 . If we choose a power-law form for $\xi(r)$ (equation (1) in Box 2), then it follows⁹⁸ that $D_2 = 3 - \gamma$ if $\xi \gg 1$. If $\xi(r) = 0$, we obtain $D_2 = 3$. The CDM models give us the correlation function $\xi(r)$ on scales greater than $\sim 10 h^{-1}$ Mpc, where we do not need to worry about nonlinear gravitational effects. The function $N(<R)$ can then be calculated from these correlations. The predicted runs of $D_2(R)$ from three different CDM models are given in Fig. 4. They may differ somewhat but they all show the same qualitative behaviour: above $30 h^{-1}$ Mpc we should be able to measure dimensions close to 3, not 2. Above $100 h^{-1}$ Mpc, they become indistinguishably close to 3. They also illustrate that it is inappropriate to quote a single crossover scale to homogeneity, for the crossover is gradual. Here we have described but one statistical fractal measure, D_2 , out of a much larger set known as the 'multifractal spectrum', which is a useful tool for the statistical description of redshift surveys⁹⁹.

Local galaxies are strongly clustered

The clumpiness of matter in the Universe was initially studied by measuring the clustering of bright galaxies^{8,9}. Figure 1 shows 2 million optically selected galaxies¹⁰ projected on the sky. The distribution is evidently not uniform: galaxies are arranged in clusters and 'filaments', and avoid certain regions termed 'voids'. Figure 2 shows data from the largest redshift survey to date, Las Campanas¹¹, which illustrates (insofar as the redshift of each galaxy indicates its distance) the three-dimensional clustering of galaxies. Although clustering is seen on scales of tens of megaparsecs, on larger scales the distribution seems more homogeneous.

It is well established that the probability of finding a galaxy

$\sim 5 h^{-1}$ Mpc away from another galaxy is twice the probability expected in a uniform distribution (Box 2). The clustering of optical galaxies^{12,13} is illustrated in Fig. 3, which shows $\langle (\delta\rho/\rho)^2 \rangle$, where ρ is the density and $\delta\rho$ is the fluctuation, as a function of characteristic length scale λ . The solid and dashed lines correspond to two variants of the cold dark matter (CDM) model for mass density fluctuations¹⁴, which is widely used as a 'template' for comparison with data. We see that the fluctuations drop monotonically with scale (although not as a pure power-law). On a scale of $\lambda \approx 100 h^{-1}$ Mpc, the root-mean-square (r.m.s.) fluctuation is only 10%. This is the crucial evidence that on larger scales the fluctuations become negligible.

It is most unlikely that luminous galaxies trace perfectly the mass distribution. Galaxies can only form in dense regions, and their formation may be affected by other physical conditions and local environment: the clustering of galaxies is therefore likely to be 'biased' relative to the mass fluctuations (Box 2). Indeed, the galaxy distribution could in principle display conspicuous features on very large scales even if the mass did not—for instance, a long cosmic string could 'seed' galaxy formation in its wake. So the galaxies could be arrayed in a fractal structure, even if the mass distribution is non-fractal. It is important therefore to understand the biasing in order to match the fluctuations in galaxies to the fluctuations in mass.

Other (biased) probes at large distances are clusters of galaxies, as selected optically by Abell¹⁵ or by X-ray surveys¹⁶. These surveys typically probe out to redshift $z \approx 0.1$. Several studies^{17,18} suggest that on scales of $\sim 600 h^{-1}$ Mpc, the distribution of Abell clusters is homogeneous.

A more controversial result on the distribution of galaxies suggests a 'characteristic scale' of clustering of $\sim 128 h^{-1}$ Mpc (refs 19, 20). It is not clear yet if this feature is real, or just due to small-number statistics or survey geometry²¹. Einasto *et al.*²² have suggested that Abell clusters lie in a quasiregular three-dimensional network of superclusters and voids, with regions of high density separated by about $120 h^{-1}$ Mpc. The reality of such a 'periodicity' in galaxy clustering should soon be revisited by two new large redshift surveys. The American–Japanese Sloan Digital Sky Survey (SDSS) should yield redshifts for about 1 million galaxies, and the Anglo–Australian '2 degree Field' (2dF) survey should produce redshifts for 250,000 galaxies (both with median redshift of $\bar{z} \approx 0.1$). These big galaxy surveys should provide good statistics on scales larger than $\sim 100 h^{-1}$ Mpc.

Tracers at high redshift

We need to observe beyond $z = 0.1$ in order to sample a big enough volume to probe clustering on scales above $\sim 300 h^{-1}$ Mpc, and to fill the gap between scales probed by galaxy surveys and the scales probed by COBE. However, this then introduces the extra complication that we cannot interpret the data without taking account of how the clustering evolves with time, and also possible cosmic evolutionary effects in the brightness of objects. The XRB and radio

Table 1 Estimates of the fractal correlation dimensions

	Sample	R (h^{-1} Mpc)	D_2
Guzzo <i>et al.</i> ⁶⁶	Perseus-Pisces	10–3.5	1.2
		3.5–20	2.2
Martinez and Coles ⁶⁷	QDOT	1.0–10	2.25
		10–50	2.77
		1.0–30	2.0
Lemson and Sanders ⁶⁸	CfA	30–60	2.7–2.9
Martínez <i>et al.</i> ⁷⁰	Stromlo-APM	300–400	2.93
Scaramella <i>et al.</i> ¹⁸	ESO Slice Project		
X-Ray background		~ 500	$3 - D_2 = 10^{-4}$, with $\sigma_\delta = 2$, $\Gamma = 0.5$
COBE 4-year normalization		$\sim 1,000$	$3 - D_2 = 2 \times 10^{-5}$, with $\sigma_\delta = 1.4$, $\Gamma = 0.5$

Some estimates of the fractal correlation dimension D_2 obtained from galaxy surveys, showing a general increase with scale R , as defined in Box 1. Scaramella *et al.*¹⁸ analysed a number of subsamples with different methods, from which we chose one of their largest. All their results that include necessary 'k-corrections', which account for the effect of galaxy spectra being redshifted relative to the observer's pass band, are consistent with $D_2 = 3$ within their errors. Also given are estimates of D_2 from the X-ray background (XRB) and the cosmic microwave background (CMB), obtained by normalizing a standard cold dark matter (CDM) model to match measured anisotropy results. Such models are characterized by the value of σ_8 , the r.m.s. fluctuation on $8 h^{-1}$ Mpc scale, and a so-called shape parameter Γ . Unlike the other measurements in this table, the CMB probes directly the fluctuations in mass.

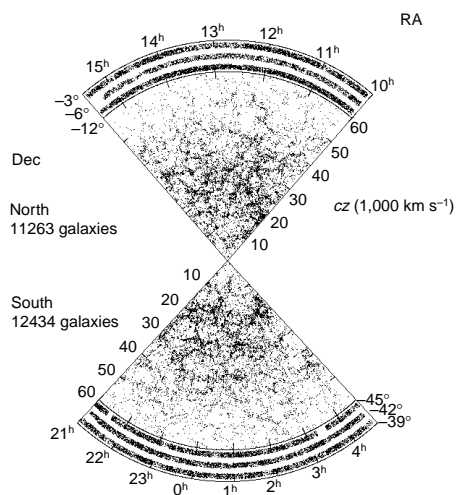


Figure 2 The redshift distribution of more than 20,000 galaxies, from the Las Campanas redshift survey¹¹. The plot shows the superposition of three slices in the north Galactic cap, and likewise for the south Galactic cap, plotted in redshift versus angular coordinates (RA, right ascension; dec., declination). Clustering of galaxies is seen on scales smaller than $\sim 30h^{-1}$ Mpc, but on larger scales the distribution approaches homogeneity. We note that the diluted density of galaxies at higher redshifts is an artefact, due to the selection of galaxies by their apparent flux.

sources are tracers of galaxies (or at least of that subset which is active) out to median redshift $\bar{z} \approx 1$. Figure 3 shows that the limits they set to large-scale inhomogeneities ($>100h^{-1}$ Mpc) are less stringent than those implied by CMB measurements; but they provide independent constraints, as they sample ‘luminous’ objects rather than the total mass. Other possible high-redshift tracers are quasars and clusters of galaxies.

Radio galaxies. Radio sources in surveys have typical median redshift $\bar{z} \approx 1$, and hence are useful probes of clustering at high redshift. Earlier studies²³ claimed that the distribution of radio sources supports the cosmological principle. However, their wide range in intrinsic luminosities would dilute any clustering when projected on the sky. Analyses of new deep radio surveys²⁴ suggest that radio sources are clustered at least as strongly as local optical galaxies^{25–31}. Nevertheless, on very large scales the distribution of radio sources seems nearly isotropic. The measured quadrupole offers a crude estimate³² of the fluctuations on scales $\lambda \approx 600h^{-1}$ Mpc. The derived amplitudes are shown in Fig. 3 for the two assumed CDM models. Given the problems of catalogue matching and shot-noise, these points should be interpreted as significant ‘upper limits’, not as detections.

The X-Ray background (XRB). Although discovered in 1962, the origin of the XRB is still controversial, but its sources, whatever they turn out to be, are likely to be at high redshift^{33,34}.

The XRB is a unique probe of fluctuations on intermediate scales between those of local galaxy surveys and COBE^{35–41}, although the interpretation of the results depends on the nature of the X-ray sources and their evolution. The r.m.s. dipole and smaller-scale fluctuations over the sky can be predicted³⁸ in the framework of gravitational instability and assumptions about the distribution of the X-ray sources with redshift. By comparing these predictions with data from HEAO⁴², it is possible to estimate the amplitude of fluctuations for an assumed shape of the density fluctuations (for example, the CDM model). Figure 3 shows the amplitude of fluctuations derived at the effective scale $\lambda \approx 600h^{-1}$ Mpc probed by the XRB. Assuming a specific epoch-dependent biasing scheme⁴³ (Box 2) and a range of models of evolution of X-ray sources and clustering, the present-epoch density fluctuations of the X-ray sources is found to be no more than twice the amplitude of fluctuations in mass⁴².

Box 2 Quantitative measures of galaxy clustering

One popular measure of galaxy clustering is the two-point correlation function⁸. This is defined as the excess probability, relative to a random distribution, of finding a galaxy at a distance r from another galaxy. It is now well established that on scales smaller than $\sim 10h^{-1}$ Mpc it has roughly the form:

$$\xi(r) = \left(\frac{r}{r_0}\right)^{-\gamma} \quad (1)$$

For optically selected galaxies, $\gamma = 1.8$ and $r_0 \approx 5h^{-1}$ Mpc; for galaxies observed in the infrared with the IRAS satellite, which include spiral galaxies but under-represent ellipticals, $r_0 \approx 4h^{-1}$ Mpc with a somewhat shallower slope⁷⁵. The clustering of galaxy clusters (as selected optically by Abell¹⁵ or by X-ray surveys) obeys a similar law⁷⁶ but with a much stronger clustering amplitude, $r_0 \approx (15\text{--}20)h^{-1}$ Mpc. The Fourier transform of the correlation function $\xi(r)$ is the power spectrum $P(k)$ (where k is the wavenumber), which corresponds to the square of Fourier coefficients of the fluctuations. The r.m.s. fluctuations (Fig. 3) can be written as $((\delta\rho/\rho)^2) \propto k^2 P(k)$.

It is not likely that the fluctuations in the density of particular galaxy types are exactly the same as the fluctuations in mass. The simplest assumption, which has been widely adopted, is that the galaxy and mass density fluctuations (δ_g and δ_m , respectively) at any point \mathbf{x} are related by;

$$\delta_g(\mathbf{x}) = b\delta_m(\mathbf{x}) \quad (2)$$

where b is the ‘bias parameter’. Usually $b > 1$, which implies that the galaxies are more clustered than the mass distribution. By modelling galaxies as peaks of the underlying mass distribution and using an argument analogous to that which explains why the highest ocean waves come in groups, Kaiser⁷⁷ showed that in the linear approximation the correlation function of galaxies (ξ_{gg}) is related to the mass correlation function (ξ_{mm}) by;

$$\xi_{gg}(r) = b^2 \xi_{mm}(r) \quad (3)$$

where r is the separation between galaxies or mass elements. We note that although equation (3) does follow from equation (2), it is more general and does not imply equation (2). Various theoretical and observational considerations suggest that $b \approx 1\text{--}2$.

Biasing must certainly be more complicated than equations (2) and (3); indeed, clustering is not the same for galaxies of different morphologies. For example, elliptical galaxies are more strongly clustered than spiral galaxies on scales $\leq 10h^{-1}$ Mpc (refs 78–80). The appropriate value of b may depend on scale, as well as on the local overdensity. Furthermore, it is not clear *a priori* that δ_g is just a function of δ_m . The efficiency of galaxy formation could in principle be modulated by some large-scale environmental effects (for example, heating by early quasars, or the proximity of a cosmic string) which are uncorrelated with δ_m . Biasing might therefore be non-local, nonlinear, stochastic and epoch-dependent^{43,45,81–87}.

Quasars, high-redshift galaxies and Lyman- α clouds. Until the mid-1990s, quasars—hyperactive galactic nuclei—were the only objects luminous enough to be identified in substantial numbers at redshifts $z > 2$. It is still unclear how their clustering evolves with redshift⁴⁴, but they appear no more clustered than extragalactic radio sources (which are a related population). The advent of 10-metre-class telescopes now allows the detection of galaxies out to equally large redshifts. Several hundred galaxies with $z \geq 3$ have already been detected, and they display about the same level of clustering as nearby galaxies⁴⁵. As gravitational effects enhance density contrasts during cosmic expansion, one might at first sight have expected weaker clustering of galaxies at earlier times. However, the luminous galaxies that have already formed at the epoch corresponding to $z = 3$ belong to an exceptional subset associated with unusually high density peaks, which display enhanced clustering (Box 2). When this is taken into account, the data are compatible with CDM models normalized to match the degree of clustering at low redshifts⁴⁵.

The rich absorption-line spectra of high-redshift quasars offer a probe for the distribution of intervening material. In particular, the ‘Lyman- α forest’ in quasar spectra reveals the distribution of diffuse gas clouds along the line of sight. There are no large ‘clearings’ in the Lyman- α forest: indeed the relevant clouds seem even more smoothly distributed than galaxies⁴⁶. Moreover, the spectra of different quasars indicate that the clouds have similar properties along all lines of sight. Relating the spacings of these clouds to the overall mass distribution (or even to the galaxy distribution) is not straightforward. However, if the clouds manifested scale-free fractal-like structure it would be remarkable if this structure were not plainly apparent in quasar absorption spectra⁷.

Direct probes of mass distribution

We have emphasized that the luminous objects selected by surveys may not trace the total mass. There are, however, at least three independent probes of inhomogeneities in the gravitational field induced by the total mass fluctuations: lensing, the CMB, and peculiar velocities. Gravitational lensing—the distortion of distant galaxy images by intervening potential wells—cannot, as yet, constrain the mass fluctuations on scales larger than $20 h^{-1}$ Mpc or so^{47,48}. Here we focus on the other two probes of mass fluctuations, which show good consistency with the picture that

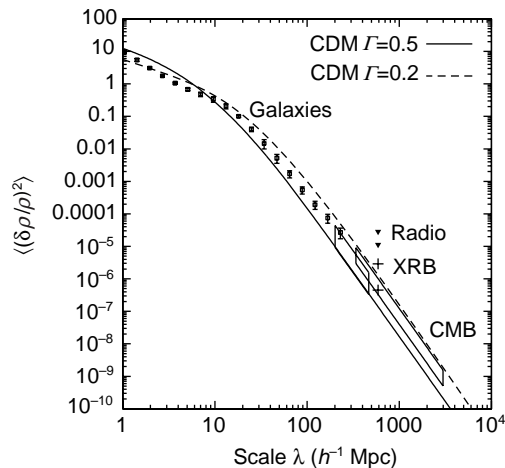


Figure 3 A compilation of density fluctuations on different scales from various observations. Shown are data from a galaxy survey, deep radio surveys, the X-ray background (XRB) and cosmic microwave background (CMB) experiments. The measurements are compared with two popular cold dark matter (CDM) models. The figure shows mean-square density fluctuations $\langle(\delta\rho/\rho)^2\rangle$. The solid and dashed lines correspond respectively to the standard CDM power spectrum (with shape parameter $\Gamma = 0.5$) and a ‘low-density’ CDM power spectrum (with $\Gamma = 0.2$). Both models are normalized such that the r.m.s. fluctuation within $8h^{-1}$ Mpc spheres is $\sigma_{8M} = 1$. The open squares at small scales are estimates of the power spectrum from three-dimensional inversion of the angular APM galaxy catalogue^{12,13}. The elongated ‘boxes’ at large scales represent the COBE 4-yr (refs 57, 90, 91) (on the right) and Tenerife⁹² (on the left) CMB measurements. The filled triangles represent constraints from the quadrupole moment of the distribution of radio sources³². This quadrupole measurement probes fluctuations on scale $\lambda_* \approx 600h^{-1}$ Mpc. The top and bottom filled triangles are upper limits of the amplitude of the power spectrum at λ_* , assuming CDM power spectra with shape parameters $\Gamma = 0.2$ and 0.5 , respectively, and an Einstein-de Sitter universe. The crosses represent constraints from the XRB HEAO1 quadrupole^{38,42}. Assuming evolution, clustering and epoch-dependent biasing prescriptions, this XRB quadrupole measurement probes fluctuations on scale $\lambda_* \approx 600h^{-1}$ Mpc, very similar to the scale probed by the radio sources. The top and bottom crosses are estimates of the amplitude of the power spectrum at λ_* , assuming CDM power spectra with shape parameters $\Gamma = 0.2$ and 0.5 , respectively, and an Einstein-de Sitter universe. The fractional error on the XRB amplitudes (due to the shot noise of the X-ray sources) is $\sim 30\%$.

amplitudes are significant on small scales but are tiny on the very large scales.

The cosmic microwave background (CMB). The CMB is well described by a black-body radiation spectrum at a temperature of 2.73 K, hence providing crucial evidence for the hot Big Bang model. This sea of radiation is highly isotropic, the main anisotropy being due to the motion of our Galaxy (the Milky Way) at 600 km s^{-1} relative to the CMB. This motion is remarkably well reconstructed in both amplitude and direction by summing up the forces due to masses represented by galaxies^{49,50} at distances nearer than $\sim 100 h^{-1}$ Mpc. The dipole anisotropy in the distribution of nearby supernovae also indicates that most of the Galaxy’s motion arises from local inhomogeneities⁵¹.

Apart from the dipole anisotropy, the other main anisotropies in the CMB radiation are imprints at the last scattering surface at redshift $z \approx 1,000$ where the primordial plasma recombined. In 1992, the COBE satellite detected fluctuations at the level of 10^{-5} on scales of 10° ; this corresponds to a present-epoch length-scale of $\sim 1,000 h^{-1}$ Mpc (Fig. 3). These tiny CMB fluctuations are attributed to ‘metric’ or ‘curvature’ fluctuations⁵² of this order in a universe which has an approximately Friedmann–Robertson–Walker (FRW) metric of space-time (corresponding to a homogeneous and isotropic universe).

On scales smaller than $1\text{--}2^\circ$, extra contributions to the temperature fluctuations arise from motions of the plasma induced by the metric fluctuations. This interaction between plasma and gravity translates to peaks in the angular power-spectrum of the temperature fluctuations^{53–56}. The angular scales of these peaks correspond to linear scales of a few hundred megaparsecs today. Several ground-based or balloon experiments are mapping small areas of sky with resolutions of $10'$ to 2° ; early in the next century, the MAP and Planck satellites should offer all-sky coverage with this resolution. The position and height of the peaks can be used to determine the cosmological parameters with very high precision^{55–58}. Moreover, the deep galaxy maps soon to be produced by the SDSS and 2dF surveys may reveal fluctuations in the galaxy distribution, at the level of a few per cent, on scales of several hundred megaparsecs; these could then be correlated with the peaks and troughs in the CMB angular fluctuation spectrum. Fluctuations probed by radio sources and the XRB on such scales can be similarly compared to the CMB (Fig. 3).

Could large-amplitude inhomogeneities along the line of sight wash out large intrinsic fluctuations in the CMB and make it look very smooth? In fact, the general effect would be merely to distort the angular distribution of the fluctuations rather than to homogenize the temperature map^{59,60}.

Peculiar velocities. Peculiar velocities (like the 600 km s^{-1} motion of our Galaxy described above) are deviations from the recession velocity that would be expected due to the smooth expansion of the Universe. The gross features of the local peculiar velocity field inferred in this way correlate well with overdensities in galaxy distribution, for example, the Virgo cluster and the Great Attractor^{61–63}, although in some regions the agreement is not perfect, perhaps due to systematic measurement errors.

Unfortunately, the distance measurement errors increase with distance, so that peculiar velocities can only be measured reliably⁶⁴ out to distances of $\sim 20 h^{-1}$ Mpc. Lauer and Postman⁶⁵ claimed that a sample of Abell clusters out to $150 h^{-1}$ Mpc is moving at $\sim 700 \text{ km s}^{-1}$ with respect to the CMB, suggesting that the CMB dipole (caused by such relative motion) is generated largely by mass concentrations beyond $\sim 100 h^{-1}$ Mpc. However, most other studies suggest bulk flows on smaller scales.

The agreement between the CMB dipole and the dipole anisotropy of relatively nearby galaxies argues in favour of large-scale homogeneity: a given overdensity $\delta\rho$ on a scale λ produces a peculiar velocity proportional to λ (in the linear regime), so a bigger peculiar velocity would be induced by larger-scale features unless $\delta\rho$ decreased as steeply as $\propto 1/\lambda$.

Large-scale structure

Although the Universe has a fractal structure on small scales, the foregoing discussion suggests that the mass distribution approaches homogeneity on large scales; that is, the fractal dimension must make a transition to $D_2 \approx 3$ (Box 1 and Fig. 4). Luminous matter does not necessarily trace mass: the galaxy distribution could in principle have been highly irregular on large scales if, for instance, galaxy formation were seeded by topological defects (for example, strings) uncorrelated with the large-scale mass distribution.

In recent years, Pietronero and co-workers³⁻⁵ have strongly advocated that the scale of homogeneity has not been detected even in the deepest redshift surveys. Most analyses of density fluctuations had assumed large-scale homogeneity, but these authors applied methods that made no such assumptions and argued that the fractal behaviour extended to the largest scales probed ($\sim 1,000 h^{-1}$ Mpc), with $D_2 \approx 2$. However, CDM models of density fluctuations (which fit reasonably well the available observational data) predict that at scales above $\sim 10 h^{-1}$ Mpc one should begin to detect values of D_2 greater than 2, with $D_2 \approx 3$ on scales larger than $\sim 100 h^{-1}$ Mpc (Box 1 and Fig. 4), in conflict with Pietronero's claim.

Several authors have therefore made further analyses of galaxy distributions using fractal algorithms^{18,66-70}. All of them obtained results which were consistent with standard models of density fluctuations, and all appeared to detect an approach to homogeneity on the largest scales analysed by them. We list some results for D_2 in Table 1. Although the statistics are still poor (and the quoted results do not all agree with each other), one can already see a steady increase towards $D_2 = 3$. In particular, the results do not support a constant D_2 for all scales, and the latest results by Scaramella *et al.*¹⁸ provide one of the closest fractal measurements yet to homogeneity. Scaramella *et al.* pointed out the importance of appropriate corrections to the observed flux from high-redshift galaxies to account for redshifting of their spectrum across the observer's waveband. These spectral band corrections are crucial to the interpretation of high-redshift photometry and should not be left out, approximate though they may be.

This debate has made a positive contribution by highlighting some technical issues. For example, it was correctly pointed out³ that if a survey is too small, then one cannot define the mean density (as the galaxies do form a fractal on small scales) and hence related tools such as correlation functions can be misleading. In analysing

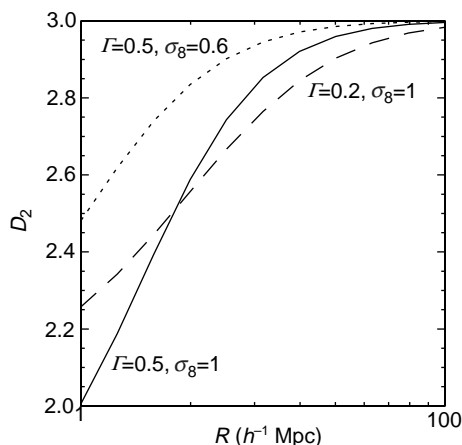


Figure 4 The fractal correlation dimension D_2 versus length scale R . The analysis assumes CDM models of power spectra with shape and normalization parameters ($\Gamma = 0.5$, $\sigma_8 = 0.6$), ($\Gamma = 0.5$, $\sigma_8 = 1.0$) and ($\Gamma = 0.2$, $\sigma_8 = 1.0$). Regardless of model, they all show the same qualitative behaviour of increasing D_2 with R , becoming vanishingly close to 3 for $R > 100 h^{-1}$ Mpc. A pure fractal model³⁻⁵ corresponds to the horizontal axis $D_2 = 2$, in conflict with CDM models and the data presented in Table 1.

local volumes within $\sim 30 h^{-1}$ Mpc, the fractal nature of clustering implies that one has to exercise caution when using statistical methods which assume homogeneity. On the other hand, the proponents of fractals have not helped their cause by using very incomplete and inhomogeneous samples. Detailed arguments for⁵ and against^{7,71,72} fractals on large scales have been given. The continued application of fractal algorithms to larger and deeper surveys should definitively resolve the matter.

The dependence of both the number counts and the angular correlation function of galaxies on apparent luminosity are strong evidence against a pure fractal universe⁹. Furthermore, because properties of a pure fractal are independent of scale, the projected galaxy distribution in shells of increasing size should look the same. This is strongly in conflict with the observations⁷, which show decreasing clumpiness in large shells. However, we note that visual impression alone cannot indicate the closeness to isotropy.

We consider that the agreement of XRB and CMB fluctuations with the popular CDM models—within the framework of a homogeneous universe—argues strongly against a pure fractal distribution for mass, or even for galaxies. (We remind the reader that the XRB traces galaxies, whereas the CMB traces mass.) Although direct estimates of D_2 are not possible on the scales probed by the XRB and the CMB, we can calculate their values by using CDM models normalized with the XRB and CMB as described above. The resulting values are extremely close to 3 and are given in the lower part of Table 1. (They are even tighter than the constraint $3 - D_2 \leq 0.001$ obtained by Peebles⁹ from the XRB using a different argument.) Can we go further? Isotropy does not imply homogeneity, but the near-isotropy of the CMB can be combined with the copernican principle that we are not in a preferred position. All observers would then measure the same near-isotropy, and it can be proved that the Universe must then be very well approximated by the FRW metric^{59,73}.

Although we reject the pure fractal model where D_2 is a constant on all scales, it remains worthwhile to explore further models that do not, *a priori*, assume gaussian fluctuations in a homogeneous background.

A common assumption is that the *metric* fluctuations—the deviations of the early universe from an exact FRW model—had the same amplitude on every scale. These fluctuations can be considered as scale-independent irregularities in the gravitational potential: ‘inflationary’ models suggest how they might have arisen, and the CMB data suggest an amplitude of about 10^{-5} . Such fluctuations would evolve into nonlinear clusters whose gravitational binding energy is $\sim 10^{-5}$ times their rest-mass energy: this corresponds to a virial velocity of $\sim 10^{-2.5}$ times the velocity of light, or $\sim 1,000 \text{ km s}^{-1}$. We do indeed observe such clusters in the present Universe. But we would expect a natural upper limit to the scale of nonlinear structures. Metric perturbations of $\sim 10^{-5}$ are too weak to have halted the expansion of regions whose boundaries are expanding, due to the Hubble flow, at much more than $1,000 \text{ km s}^{-1}$: they would merely have induced slight perturbations in density, with amplitude inversely proportional to the square of the scale. If the present-day *density* fluctuations in the cosmic mass distribution were scale-independent, the associated potential (or metric) fluctuations would increase as the square of the scale. It seems clear that we do not live in such a universe: it is, on the contrary, the initial fluctuations in the *metric* (rather than in the mass density) that are scale-independent. This would not formally preclude a simple fractal distribution of luminous objects, if these did not ‘track’ the overall mass distribution; we have, however, shown that galaxies, radio sources and the sources of the XRB have a distribution that becomes smoother as we average over larger scales. Of course, we still cannot formally exclude a pre-copernican model universe, such that the isotropy around us is atypical of what would be measured by hypothetical observers elsewhere⁷⁴. But, leaving such matters aside, there is a well defined sense in which our Universe is

homogeneous on the largest accessible scales; neither its mass distribution, nor that of the galaxies, resembles a pure fractal. Cosmological parameters such as Ω therefore have a well defined meaning—indeed these considerations tell us over what volume we need to average in order to determine them with any specified level of precision. \square

K.K.S.W. and M.J.R. are at the Institute of Astronomy, University of Cambridge, Madingley Road, Cambridge CB3 0HA, UK. O.L. is at the Racah Institute of Physics, The Hebrew University, Jerusalem 91904, Israel and at the Institute of Astronomy, University of Cambridge, Cambridge, UK.

1. Mandelbrot, B. B. *The Fractal Geometry of Nature* (Freeman, New York, 1983).
2. Mandelbrot, B. B. in *Current Topics in Astrofundamental Physics: Primordial Cosmology* (eds Sánchez, N. & Zichichi, A.) 583–602 (Kluwer, Dordrecht, 1998).
3. Coleman, P. H., Pietronero, L. & Sanders, R. H. Absence of any characteristic correlation length in the CfA galaxy catalogue. *Astron. Astrophys.* **200**, L32–L34 (1988).
4. Pietronero, L., Montuori, M. & Sylos-Labini, F. On the fractal structure of the visible universe. In *Critical Dialogues in Cosmology* (ed. Turok, N.) 24–49 (World Scientific, Singapore, 1997).
5. Sylos Labini, F., Montuori, M. & Pietronero, L. Scale-invariance of galaxy clustering. *Phys. Rep.* **293**, 61–226 (1998).
6. Borgani, S. Scaling in the universe. *Phys. Rep.* **251**, 2–152 (1995).
7. Davis, M. Is the universe homogeneous on large scales? In *Critical Dialogues in Cosmology* (ed. Turok, N.) 13–23 (World Scientific, Singapore, 1997).
8. Peebles, P. J. E. *The Large-Scale Structure of the Universe* (Princeton Univ. Press, 1980).
9. Peebles, P. J. E. *Principles of Physical Cosmology* (Princeton Univ. Press, 1993).
10. Maddox, S. J., Efstathiou, G., Sutherland, W. J. & Loveday, J. Galaxy correlations on large scales. *Mon. Not. R. Astron. Soc.* **242**, 43P–47P (1990).
11. Shectman, S. A. et al. The Las Campanas Redshift Survey. *Astron. Astrophys. J.* **470**, 172–188 (1996).
12. Baugh, C. M. & Efstathiou, G. The three-dimensional power spectrum measured from the APM Galaxy Survey-1. Use of the angular correlation function. *Mon. Not. R. Astron. Soc.* **265**, 145–156 (1993).
13. Baugh, C. M. & Efstathiou, G. The three-dimensional power spectrum measured from the APM Galaxy Survey-2. Use of the two-dimensional power spectrum. *Mon. Not. R. Astron. Soc.* **267**, 323–332 (1994).
14. Bardeen, J. M., Bond, J. R., Kaiser, N. & Szalay, A. S. The statistics of peaks of Gaussian random fields. *Astron. Astrophys. J.* **304**, 15–61 (1986).
15. Abell, G. O. The distribution of rich clusters of galaxies. *Astron. Astrophys. J. Suppl.* **3**, 211–288 (1958).
16. Ebeling, H. et al. Properties of the X-ray-brightest Abell-type clusters of galaxies (XBACs) from ROSAT All-Sky Survey data-1. The sample. *Mon. Not. R. Astron. Soc.* **281**, 799–829 (1996).
17. Scaramella, R. Mass fluctuations on 600/h Mpc—A result from clusters of galaxies. *Astron. Astrophys. J.* **390**, L57–L60 (1992).
18. Scaramella, R. et al. The ESO Slice Project [ESP] galaxy redshift survey. V. Evidence for a D=3 sample dimensionality. *Astron. Astrophys. J.* **334**, 404–408 (1998).
19. Broadhurst, T. J., Ellis, R. S., Koo, D. C. & Szalay, A. S. Large-scale distribution of galaxies at the Galactic poles. *Nature* **343**, 726–728 (1990).
20. Landy, S. D. et al. The two-dimensional power spectrum of the Las Campanas Redshift Survey: Detection of excess power on 100 h⁻¹ Mpc scales. *Astron. Astrophys. J.* **456**, L1–L4 (1996).
21. Kaiser, N. & Peacock, J. A. Power-spectrum analysis of one-dimensional redshift surveys. *Astron. Astrophys. J.* **379**, 482–506 (1991).
22. Einasto, J. et al. A 120-Mpc periodicity in the three-dimensional distribution of galaxy superclusters. *Nature* **385**, 139–141 (1997).
23. Webster, A. The clustering of radio sources. I—The theory of power-spectrum analysis. II—The 4C, GB and MC1 surveys. *Mon. Not. R. Astron. Soc.* **175**, 61–83 (1976).
24. Condon, J. J. in *New Horizons from Multi-wavelength Sky Surveys* (eds McLean, B. J. et al.) 19–25 (Proc. IAU Symp. 179, Kluwer, Dordrecht, 1998).
25. Shaver, P. A. & Pierre, M. Large-scale anisotropy in the sky distribution of extragalactic radio sources. *Astron. Astrophys. J.* **220**, 35–41 (1989).
26. Benn, C. R. & Wall, J. V. Structure on the largest scales: constraints from the isotropy of radio source counts. *Mon. Not. R. Astron. Soc.* **272**, 678–698 (1995).
27. Koorman, B. L., Burns, J. O. & Klypin, A. A. Two-point angular correlation function for the Green Bank 4.85 GHz Sky Survey. *Astron. Astrophys. J.* **448**, 500–509 (1995).
28. Scitote, H. *Large-scale Clustering of Radio Sources from the Green Bank 1987 Survey*. Thesis, Princeton Univ. (1995).
29. Loan, A. J., Wall, J. V. & Lahav, O. The correlation function of radio sources. *Mon. Not. R. Astron. Soc.* **286**, 994–1002 (1997).
30. Cress, C. M., Helfand, D. J., Becker, R. H., Gregg, M. D. & White, R. L. The angular two-point correlation function for the FIRST radio survey. *Astron. Astrophys. J.* **473**, 7–14 (1996).
31. Magliocchetti, M., Maddox, S. J., Lahav, O. & Wall, J. V. Variance and skewness in the FIRST survey. *Mon. Not. R. Astron. Soc.* **300**, 257–268 (1998).
32. Baleisis, A., Lahav, O., Loan, A. J. & Wall, J. V. Searching for large scale structure in deep radio surveys. *Mon. Not. R. Astron. Soc.* **297**, 545–558 (1998).
33. Boldt, E. A. The cosmic X-ray background. *Phys. Rep.* **146**, 215–257 (1987).
34. Fabian, A. C. & Barcons, X. The origin of the X-ray background. *Annu. Rev. Astron. Astrophys.* **30**, 429–456 (1992).
35. Rees, M. in *Objects of High Redshift* (eds Abell, G. O. & Peebles, P. J. E.) 207–224 (Proc. IAU Symp. 92, Reidel, Dordrecht, 1980).
36. Shafer, R. A. *Spatial Fluctuations in the Diffuse Cosmic X-ray Background*. Thesis, NASA Goddard Space Flight Center (1983).
37. Boughn, S. P., Crittenden, R. G. & Turok, N. G. Correlations between the cosmic X-ray and microwave backgrounds: constraints on a cosmological constant. *New Astron.* **3**, 275–291 (1998).
38. Lahav, O., Piran, T. & Treyer, M. A. The X-ray background as a probe of density fluctuations at high redshift. *Mon. Not. R. Astron. Soc.* **284**, 499–506 (1997).
39. Barcons, X., Fabian, A. C. & Carrera, F. J. Measuring the power spectrum of density fluctuations at intermediate redshift with X-ray background observations. *Mon. Not. R. Astron. Soc.* **293**, 60–70 (1998).
40. Jahoda, K. Present epoch plus—an X-ray survey for cosmology. *Astron. Nachrichten* **319**, 129–132 (1998).
41. Boughn, S. P. Cross-correlation of the 2–10 keV X-ray background with radio sources: Constraining the large-scale structure of the X-ray background. *Astron. Astrophys. J.* **499**, 533–541 (1998).
42. Treyer, M. et al. Large scale fluctuations in the X-Ray Background. *Astron. Astrophys. J.* **509**, 531–536 (1998).
43. Fry, J. N. The evolution of bias. *Astron. Astrophys. J.* **461**, L65–L68 (1996).
44. Shanks, T. & Boyle, B. J. QSO clustering—I. Optical surveys in the redshift range 0.3 < z < 2.2. *Mon. Not. R. Astron. Soc.* **271**, 753–772 (1994).
45. Steidel, C. C. et al. A large structure of galaxies at redshift z approximately 3 and its cosmological implications. *Astron. Astrophys. J.* **492**, 428–438 (1998).
46. Webb, J. K. & Barcons, X. A search for inhomogeneities in the Lyman-alpha forest. *Mon. Not. R. Astron. Soc.* **250**, 270–277 (1991).
47. Villumsen, J. V. Weak lensing by large-scale structure in open, flat and closed universes. *Mon. Not. R. Astron. Soc.* **281**, 369–383 (1996).
48. Kaiser, N. Weak lensing and cosmology. *Astron. Astrophys. J.* **498**, 26–42 (1998).
49. Strauss, M. A., Yahil, A., Davis, M., Huchra, J. P. & Fisher, K. A redshift survey of IRAS galaxies. V—The acceleration on the Local Group. *Astron. Astrophys. J.* **397**, 395–419 (1992).
50. Webster, M., Lahav, O. & Fisher, K. Wiener reconstruction of the IRAS 1.2-Jy galaxy redshift survey: cosmographical implications. *Mon. Not. R. Astron. Soc.* **287**, 425–444 (1997).
51. Riess, A. G., Davis, M., Baker, J. & Kirshner, R. P. The velocity field from type Ia supernovae matches the gravity field from galaxy surveys. *Astron. Astrophys. J.* **488**, L1–L6 (1997).
52. Sachs, R. K. & Wolfe, A. M. Perturbations of a cosmological model and angular variations of the microwave background. *Astron. Astrophys. J.* **147**, 73–90 (1967).
53. White, M., Scott, D. & Silk, J. Anisotropies in the cosmic microwave background. *Annu. Rev. Astron. Astrophys.* **32**, 319–370 (1994).
54. Scott, D., Silk, J. & White, M. From microwave anisotropies to cosmology. *Science* **268**, 829–835 (1995).
55. Hu, W., Sugiyama, N. & Silk, J. The physics of microwave background anisotropies. *Nature* **386**, 37–43 (1997).
56. Bennett, C. L., Turner, M. S. & White, M. The cosmic rosetta stone. *Phys. Today* **50**, 32–38 (1997).
57. Gawiser, E. & Silk, J. Extracting primordial density fluctuations. *Science* **280**, 1405–1411 (1998).
58. Webster, M. et al. Joint estimation of cosmological parameters from CMB and IRAS data. *Astron. Astrophys. J.* **509**, L65–L68 (1998).
59. Stoeger, W. R., Maartens, R. & Ellis, G. F. R. Proving almost-homogeneity of the universe: An almost Ehlers-Green-Sachs theorem. *Astron. Astrophys. J.* **443**, 1–5 (1995).
60. Seljak, U. Gravitational lensing effect on cosmic microwave background anisotropies: A power spectrum approach. *Astron. Astrophys. J.* **463**, 1–7 (1996).
61. Lynden-Bell, D. et al. Spectroscopy and photometry of elliptical galaxies. V—galaxy streaming toward the new supergalactic center. *Astron. Astrophys. J.* **326**, 19–49 (1988).
62. Dekel, A. Dynamics of cosmic flows. *Annu. Rev. Astron. Astrophys.* **32**, 371–418 (1994).
63. Strauss, M. A. & Willick, J. A. The density and peculiar velocity fields of nearby galaxies. *Phys. Rep.* **261**, 271–431 (1995).
64. Kolatt, T. & Dekel, A. Large-scale power spectrum from peculiar velocities. *Astron. Astrophys. J.* **479**, 592–605 (1997).
65. Lauer, T. R. & Postman, M. The motion of the Local Group with respect to the 15000 kilometer per second Abell cluster inertial frame. *Astron. Astrophys. J.* **425**, 418–438 (1994).
66. Guzzo, L., Iovino, A., Chincarini, G., Giovanelli, R. & Haynes, M. P. Scale-invariant clustering in the large-scale distribution of galaxies. *Astron. Astrophys. J.* **382**, L5–L9 (1991).
67. Martínez, V. J. & Coles, P. Correlations and scaling in the QDOT redshift survey. *Astron. Astrophys. J.* **437**, 550–555 (1994).
68. Lemson, G. & Sanders, R. H. On the use of the conditional density as a description of galaxy clustering. *Mon. Not. R. Astron. Soc.* **252**, 319–328 (1991).
69. Cappi, A., Benoist, C., Da Costa, L. N. & Maurogordato, S. Is the Universe a fractal? Results from the Southern Sky Redshift Survey 2. *Astron. Astrophys. J.* **335**, 779–788 (1998).
70. Martínez, V. J., Pons-Borderia, M.-J., Moyeed, R. A. & Graham, M. J. Searching for the scale of homogeneity. *Mon. Not. R. Astron. Soc.* **298**, 1212–1222 (1998).
71. Guzzo, L. Is the universe homogeneous? (On large scales). *New Astron.* **2**, 517–532 (1997).
72. Calzetti, D., Gialavisco, M., Ruffini, R., Taraglio, S. & Bahcall, N. A. Clustering of galaxies: Fractal or homogeneous infrastructure? *Astron. Astrophys.* **245**, 1–6 (1991).
73. Maartens, R., Ellis, G. F. R. & Stoeger, W. R. Anisotropy and inhomogeneity of the universe from $\Delta T/T$. *Astron. Astrophys. J.* **309**, L7–L10 (1996).
74. Ellis, G. F. R. Alternatives to the Big Bang. *Annu. Rev. Astron. Astrophys.* **22**, 157–184 (1984).
75. Saunders, W., Rowan-Robinson, M. & Lawrence, A. The spatial correlation function of IRAS galaxies on small and intermediate scales. *Mon. Not. R. Astron. Soc.* **258**, 134–146 (1992).
76. Bahcall, N. A. Large-scale structure in the universe indicated by galaxy clusters. *Annu. Rev. Astron. Astrophys.* **26**, 631–686 (1988).
77. Kaiser, N. On the spatial structures of Abell clusters. *Astron. Astrophys. J.* **284**, L9–L12 (1984).
78. Dressler, A. Galaxy morphology in rich clusters—Implications for the formation and evolution of galaxies. *Astron. Astrophys. J.* **236**, 351–365 (1980).
79. Loveday, J., Maddox, S. J., Efstathiou, G. & Peterson, B. A. The Stromlo-APM redshift survey. 2: Variation of galaxy clustering with morphology and luminosity. *Astron. Astrophys. J.* **442**, 457–468 (1995).
80. Hermit, S. et al. The two-point correlation function and morphological segregation in the Optical Redshift Survey. *Mon. Not. R. Astron. Soc.* **283**, 709–720 (1996).
81. Dekel, A. & Rees, M. J. Physical mechanisms for biased galaxy formation. *Nature* **326**, 455–462 (1987).
82. Babul, A. & White, S. D. M. Quasar-modulated galaxy clustering in a cold dark matter universe. *Mon. Not. R. Astron. Soc.* **253**, 31P–34P (1991).
83. Coles, P. Galaxy formation with a local bias. *Mon. Not. R. Astron. Soc.* **262**, 1065–1075 (1993).
84. Bower, R. G., Coles, P., Frenk, C. S. & White, S. D. M. Cooperative galaxy formation and large-scale structure. *Astron. Astrophys. J.* **405**, 403–412 (1993).
85. Kauffmann, G., Nusser, A. & Steinmetz, M. Galaxy formation and large-scale bias. *Mon. Not. R. Astron. Soc.* **286**, 795–811 (1997).
86. Bagla, J. Evolution of galaxy clustering. *Mon. Not. R. Astron. Soc.* **299**, 417–424 (1998).
87. Dekel, A. & Lahav, O. Stochastic nonlinear galaxy biasing. *Astron. Astrophys. J.* (in the press); also as preprint astro-ph/9806193 at (<http://xxx.lanl.gov>) (1998).
88. Szalay, A. S. & Schramm, D. N. Are galaxies more strongly correlated than clusters? *Nature* **314**, 718–719 (1985).
89. Martínez, V. J., Jones, B. J. T., Dominguez-Tenreiro, R. & Van De Weygaert, R. Clustering parameters and multifractal measures. *Astron. Astrophys. J.* **357**, 50–61 (1990).
90. Smoot, G. F. et al. Structure in the COBE differential microwave radiometer first-year maps. *Astron. Astrophys. J.* **396**, L1–L5 (1992).
91. Bennett, C. L. et al. Four-year COBE DMR cosmic microwave background observations: maps and basic results. *Astron. Astrophys. J.* **464**, L1–L4 (1996).
92. Hancock, S. et al. Studies of cosmic microwave background structure at Dec.=+40 deg - II. Analysis and cosmological interpretation. *Mon. Not. R. Astron. Soc.* **289**, 505–514 (1997).

Acknowledgements. We thank A. Baleisis, E. Gawiser, L. Guzzo and M. Treyer for discussions.

Correspondence and requests for materials should be addressed to K.K.S.W. (e-mail: kwu@ast.cam.ac.uk).